

The mutual diffusion coefficient for the van der Waals binary mixture of type I

R. Castillo, C. Garza, and H. Dominguez

Instituto de Física. UNAM., P.O. Box 20-364 Mexico, D.F. 01000 Mexico

(Received 16 April 1993; accepted 10 September 1993)

In the framework of the mean-field kinetic variational theory, the explicit dependence of the mutual diffusion coefficient of the van der Waals binary mixture with composition and interaction parameters is obtained. The different kinds of behavior shown by this coefficient can be classified according to the scheme of van Konynenburg and Scott devised to describe the global phase diagram of this model mixture. A numerical study to understand the concentration dependence of the mutual diffusion coefficients for mixtures of type I is presented here, in terms of molecular masses, sizes, and interaction parameters. Moreover, the behavior of the mutual diffusion coefficient of the van der Waals mixture is compared with that of a hard-sphere mixture. In addition, a comparison is made between our calculations and experimental data of binary systems classified as belonging to type I: H₂O/D₂O, hexane/heptane, toluene/hexane, and benzene/hexane. From the explicit model presented here, one can obtain semiquantitative explanations of the role played by the variables that determine the concentration dependence of the mutual diffusion coefficient.

I. INTRODUCTION

The mutual diffusion coefficient (MDC) measures the rate at which the concentration fluctuations (gradients) in a solution approach their equilibrium values. Therefore, the decay of these gradients to obtain the equalization of the concentration throughout the binary mixture takes place by direct change of the composition of every small portion of the fluid. The thermodynamic theory of interdiffusion has provided unequivocal statements concerning the minimum number of independent coefficients required to describe the mass transport in an isothermal fluid containing any specified number of components.¹ In some binary systems within this framework, it is possible to demonstrate some regularities in the diffusion behavior of a series of related solutes in the same solvent.² But, from a more fundamental point of view, theory has not been able to explain how the MDC is related to the intermolecular interaction parameters. Although some developments have been presented,³⁻¹⁰ the interpretation of diffusion coefficients of binary mixtures in a more fundamental way has been pursued for a long time without great success.

Probably, one of the most used theories to correlate mutual diffusion data relies on the empirical equations of Hartley and Crank.^{3,4,6,10} Here the MDC is related to two self-diffusion coefficients and it can be helpful in some applications,^{6,11} but these equations provide little insight into the nature of mutual diffusion at a microscopic level. Moreover, to be useful as a predictive tool two self-diffusion coefficients measurements are required, each of which is nearly as difficult to make as the direct measurement of the MDC itself. Hence, this approach has little value for predicting MDCs. Another approach used to correlate mutual diffusion data is the rough hard-sphere theory.^{7,8} Here a hard-sphere theory, the so-called standard Enskog theory¹² (SET), is amended to allow for the transfer of angular momentum through the rough hard-sphere

concept developed by Chandler.¹³ This theory although quite popular¹⁴⁻¹⁷ is incorrect. It relies on the standard Enskog theory which is at odds with linear irreversible thermodynamics.¹⁸ A further development in kinetic theory due to van Beijeren and Ernst¹⁹ gave rise to a corrected version for the Enskog theory, the revised Enskog theory (RET). The partial success of the rough hard-sphere theory for predicting diffusion in binary solutions, nearly ideal, arises from the way in which it includes the correction due to correlated motion. A density dependent correction factor,^{7,8} coming from comparing SET and molecular dynamics simulations²⁰ is used. Therefore, other effects in addition to correlated motion are included in this correction factor.

The RET is prominent for transport properties, since it is a kinetic theory for hard-sphere fluids, beyond the low density limit, that can give explicit calculations.^{21,22} The first computer simulation studies to test the predictions for the mutual diffusion coefficients given in the RET have been presented recently by Erpenbeck.^{23,24} In the most extended work,²⁴ that author studied equimolar mixtures having a diameter ratio of 0.4, a mass ratio of 0.03, and at volumes 5, 10, and 20 times the close-packed volume. He found evidence of negative deviations from the RET at low densities. Notwithstanding those studies, it is still an open question if the RET can predict correctly the MDC for binary mixtures of hard spheres, in particular at high densities. More simulation studies are needed to understand the contribution of correlated motion to the MDC in hard-sphere mixtures.

In binary liquid systems with a somewhat realistic intermolecular model potential, simulations of one particle dynamic phenomena are frequently studied to yield self-diffusion, but investigations of collective properties in such systems as the MDC are scarce. Hence, it is difficult to obtain a clear view of the role played by the several parameters that influence the MDC values. The best model

potential studied has been the Lennard-Jones potential.²⁵⁻³¹ The work of Hoheisel and collaborators²⁹⁻³¹ has been particularly important to understand how the particle volumes and the interaction strength affect the MDC for equimolar mixtures, as well as the role of cross correlation.

The purpose of this paper is to present an alternative route to study the mutual diffusion coefficient of binary mixtures. Of course, a point of interest here is to understand the effect on the MDC due to molecular masses, short-range forces (molecular volumes), and attractive potential interactions. There are a few model mixtures for which theory can be handled almost without approximations, and can give explicit equations relating their molecular parameters to the MDC. One of these is the van der Waals binary mixture. Hence, this paper is addressed to study the MDC of that model mixture, and to show how this procedure can be helpful to understand the way in which the interaction parameters affect the concentration dependence of the MDC of actual systems.

More than a century ago, van der Waals developed a simple model which turned out to be extremely fruitful in describing the main properties of realistic fluids. In modern language, a rigorous formulation of this model can be given by writing the molecular pair interaction in the form

$$V(r) = V^S(r) + \gamma^3 V^L(\gamma r), \quad (1)$$

where V^S refers to the short-range reference system, while V^L is the long-range part of the potential, with range γ^{-1} . If the properties of this model are analyzed in the limit of $\gamma \rightarrow 0$, the van der Waals equation combined with the Maxwell equal-area construction is obtained.³² Besides, the van der Waals theory has been developed to understand fluid phase equilibria in binary mixtures, and it has revealed a rich variety of behaviors accounting in a qualitatively way, for most of the types of fluid phase equilibria shown by actual mixtures.^{33,34} This model potential has been also used to understand a long list of related problems such as the theory of capillarity,³⁵ nonuniform fluids,³⁶ interphase properties,³⁷ and density fluctuations.³⁸

There are several points of departure to study the mutual diffusion of the van der Waals mixtures,³⁹⁻⁴³ although, the best suited for obtaining explicit expressions for the MDC in terms of molecular parameters is the mean-field kinetic variational theory.⁴³ Here the expression for the MDC is given in such a way that it can be related to the curvature of the free energy of the binary mixture. The free energy curvature in a binary mixture is responsible of the specific characteristics of the equilibrium phase diagrams. The multiplicity of phases and the connectivity of their associated critical points are determined by the form of the spinodal surfaces (free energy curvature=0). The different kinds of phase diagrams obtained for the van der Waals mixture have been classified according to a scheme devised by van Konynenburg and Scott.³³ With this classification, these authors were able to reproduce most of the known types of fluid-fluid phase equilibria observed in actual fluid mixtures. The relation between the free energy curvature and the MDC can give us a useful way to describe the global behavior of mutual diffusion on the same basis as in

phase diagrams. The behavior of the MDC is similar to that of the free energy curvature, except that the MDC is modulated by a compressibility factor,^{43,44} and factors related to the dynamics of a two-particle collision. Although, a preliminary survey using these ideas relating diffusion and phase diagram have been presented by one of us elsewhere,⁴⁴ they are neither critically discussed nor confronted with actual systems.

An outline of the paper is as follows. In Sec. II, we review the kinetic variational theory I, i.e., the van der Waalsian theory of transport processes. In Sec. III, the main features of the scheme of van Konynenburg and Scott are reviewed. Section IV is devoted to presenting a numerical study to understand how the different parameters involved in the van der Waals theory affect the concentration dependence of the MDC. In addition here, the differences between the calculations using the van der Waals theory and the RET are discussed. In Sec. V, calculations are presented for several actual systems belonging to the diagrams of type I: H₂O/D₂O, hexane/heptane, toluene/hexane and benzene/hexane. These calculations are compared with experimental data and with similar calculations performed with the RET.

II. KINETIC VARIATIONAL THEORY

The kinetic variational theory is defined by a set of coupled nonlinear mean-field kinetic equations given below, first obtained by Karkheck *et al.*⁴³ They were derived for a system of particles interacting through a pair potential consisting of a hard-sphere part plus a smooth but, otherwise arbitrary attractive tail. The set of equations for the two single particle distribution functions defined in a binary mixture $f_i(\mathbf{r}_1, \mathbf{v}_1, t)$, ($i=1,2$), are the following:

$$\begin{aligned} & \left[\frac{\partial}{\partial t} + \mathbf{v}_1 \cdot \frac{\partial}{\partial \mathbf{r}_1} \right] f_1(\mathbf{r}_1, \mathbf{v}_1, t) \\ &= C^{\text{RET}}(f_i, f_j) + \frac{1}{m_i} \sum_{j=1}^2 \int_{r_{12} > \sigma_{ij}}^{\infty} d\mathbf{r}_2 n_j(\mathbf{r}_2, t) g_{ij}^{\text{HS}}(\mathbf{r}_1, \mathbf{r}_2) \\ &+ \sigma_{ij} \epsilon \{n_k\} \frac{\partial}{\partial \mathbf{r}_1} \varphi_{ij}^{\text{tail}}(r_{12}) \cdot \frac{\partial}{\partial \mathbf{v}_1} f_i(\mathbf{r}_1, \mathbf{v}_1, t), \quad (2) \end{aligned}$$

where $f_i(\mathbf{r}_1, \mathbf{v}_1, t)$ is the average number of particles of component i (with mass m) at the position \mathbf{r}_1 , at the velocity \mathbf{v}_1 , and at the time t . $n_i = \int d\mathbf{v}_1 f_i(\mathbf{r}_1, \mathbf{v}_1, t)$.

The Kac limit

$$\varphi_{ij}^{\text{tail}} = \lim_{\gamma \rightarrow 0} \gamma^3 V_{ij}(\gamma r), \quad (3)$$

can be done in the mean field term ($\sigma_{ij} \rightarrow 0, g_{ij} \rightarrow 1$), and a kinetic equation can be obtained that embodies the exact thermodynamic description⁴³ of a system interacting with a potential consisting of a hard-sphere core, and an infinitely weak long-range attraction, i.e., the van der Waals interaction. We shall call this theory KVT I.⁴⁵ The collision term C^{RET} has exactly the form of that which appears in the revised Enskog theory introduced by van Beijeren and Ernst,¹⁹

$$C^{\text{RET}}(f_i, f_j) = \sum_{j=1}^2 \sigma_{ij}^2 \int d\mathbf{v}_2 \int d\hat{\mathbf{e}} (\hat{\mathbf{e}} \cdot \mathbf{v}_{ji}) \Theta(\hat{\mathbf{e}} \cdot \mathbf{v}_{ji}) [g_{ij}^{\text{HS}}(\mathbf{r}_1, \mathbf{r}_1 + \sigma_{ij} \hat{\mathbf{e}} | \{n_k\}) f_i(\mathbf{r}_1, \mathbf{v}'_1, t) f_i(\mathbf{r}_1 + \sigma_{ij} \hat{\mathbf{e}}, \mathbf{v}'_2, t) - g_{ij}(\mathbf{r}_1, \mathbf{r}_1 - \sigma_{ij} \hat{\mathbf{e}} | \{n_k\}) f_i(\mathbf{r}_1, \mathbf{v}_1, t) f_i(\mathbf{r}_1 - \sigma_{ij} \hat{\mathbf{e}}, \mathbf{v}_2, t)]. \quad (4)$$

Here $\mathbf{v}_{ji} = \mathbf{v}_j - \mathbf{v}_i$ is the relative velocity of two particles with velocities \mathbf{v}_j and \mathbf{v}_i , respectively. $\hat{\mathbf{e}}$ is a unit vector directed along the line of centers from the particle of component j to the particle of component i upon collision, and Θ is the Heaviside step function. \mathbf{v}'_i and \mathbf{v}'_j denote the velocities of the restituting collision, which are connected to those of the direct collision \mathbf{v}_i and \mathbf{v}_j by the relations

$$\begin{aligned} \mathbf{v}'_i &= \mathbf{v}_i + 2M_{ji}(\mathbf{v}_{ji} \cdot \hat{\mathbf{e}}) \hat{\mathbf{e}}, \\ \mathbf{v}'_j &= \mathbf{v}_j - 2M_{ij}(\mathbf{v}_{ij} \cdot \hat{\mathbf{e}}) \hat{\mathbf{e}}, \end{aligned} \quad (5)$$

where $M_{ij} = m_i/(m_i + m_j)$. The g_{ij}^{HS} s are the radial distribution functions of a binary hard-sphere mixture. They are the same functionals of the local number densities $\{n_i\}$, as in the case of the binary mixture in nonuniform equilibrium.¹⁹

Explicit expressions for the transport coefficients up to

the Navier–Stokes level can be directly obtained by expanding the heat, the momentum and the mass fluxes to linear order in the gradients. This is done by solving Eqs. (2) in the Kac limit, in the form $f_i^{(1)} = f_i^{(0)} [1 + \Phi_i]$ via the Chapman–Enskog development.¹² Here the $f_i^{(0)}$ are the local Maxwell distribution functions, and $\Phi_i = \mathcal{O}(\nabla)$. The thermal conductivity and the viscosities obtained are identical to those given in the RET.⁴³ The diffusion coefficients are the only ones that exhibit explicit dependence on the tail strength.⁴³

We will limit our derivation to the case of the MDC of a binary mixture. Here an explicit derivation to obtain this coefficient will be presented on the basis of the procedure developed by Lopez de Haro *et al.*²¹ for the case of hard spheres. The starting point for our discussion will be the linearized integral equations given for the Φ_i 's in Ref. 43

$$\begin{aligned} & \sum_{j=1}^2 \sigma_{ij}^2 y_{ij} f_i^{(0)} \int d\mathbf{v}_2 f_j^{(0)} \int d\hat{\mathbf{e}} (\hat{\mathbf{e}} \cdot \mathbf{v}_{ji}) \Theta(\hat{\mathbf{e}} \cdot \mathbf{v}_{ji}) [\Phi_j(\mathbf{v}'_2) + \Phi_i(\mathbf{v}'_1) - \Phi_j(\mathbf{v}_2) \\ & - \Phi_i(\mathbf{v}_1)] = f_i^{(0)} \left\{ (\mathbf{v}_1 - \mathbf{u}) \cdot \left[\frac{n}{n_i} \mathbf{d}_i + \frac{\partial}{\partial \mathbf{r}} \ln T \left[\mathcal{C}_i^2 - \frac{5}{2} \right] \left[1 + \left(\frac{8\pi}{5} \right) \sum_{j=1}^2 \sigma_{ij}^3 y_{ij} n_j \mu_{ij} / m_{ij} \right] + 2\mathcal{C}^{\circ} \mathcal{C} : \frac{\partial}{\partial \mathbf{r}} \mathbf{u} \right. \right. \\ & \left. \left. \times \left[1 + \left(\frac{8\pi}{15} \right) \sum_{j=1}^2 \sigma_{ij}^3 y_{ij} n_j \mu_{ij} / m_{ij} \right] + 2/3 \left[\mathcal{C}_i^2 - \frac{3}{2} \right] \frac{\partial}{\partial \mathbf{r}} \cdot \mathbf{u} \left[1 + \frac{P^{\text{HS}}}{nkT} + \left(\frac{4\pi}{3} \right) \sum_{j=1}^2 \sigma_{ij}^3 y_{ij} n_j \mu_{ij} / m_{ij} \right] \right\}. \end{aligned} \quad (6)$$

The y_{ij} are the contact values of g_{ij}^{eq} , $\mathcal{C}_i = \sqrt{m_i/2kT}(\mathbf{v}_i - \mathbf{u})$, $m_{ij} = m_i + m_j$, and $\mathcal{C}_i \mathcal{C}_i = \mathcal{C}_i^{\circ} \mathcal{C}_i^{\circ} - (1/3) \mathcal{C}_i^{\circ} \hat{\mathbf{I}}^{\circ} \hat{\mathbf{I}}^{\circ}$, $\hat{\mathbf{I}}$ being the unit dyadic and \mathbf{u} the local velocity. k is the Boltzmann constant. $\mathbf{d}_i = \mathbf{d}_i^{\text{HS}} + \mathbf{d}_i^t$, where

$$\mathbf{d}_i^{\text{HS}} = (n_i/n) \left\{ \beta \left(\frac{\partial}{\partial \mathbf{r}} \mu_i^{\text{HS}} \right)_T - \beta \left(\frac{m_i}{\rho} \right) \left(\frac{\partial}{\partial \mathbf{r}} P^{\text{HS}} \right) + \left(\frac{\partial}{\partial \mathbf{r}} \ln T \right) \left[1 + (4\pi/3) \sum_{j=1}^2 \sigma_{ij}^3 y_{ij} n_j m_i / m_{ij} \right] \right\}, \quad (7)$$

and

$$\mathbf{d}_i^t = (n_i/n) \beta \left[2 \sum_{j=1}^2 a_{ij} \frac{\partial}{\partial \mathbf{r}} n_j - \left(\frac{m_i}{\rho} \right) \frac{\partial}{\partial \mathbf{r}} P^t \right]. \quad (8)$$

Here the total number density is $n = \sum_{i=1}^2 n_i$, $\rho = \sum_{i=1}^2 n_i m_i = \sum_{i=1}^2 \rho_i$, $\beta = 1/(kT)$, the temperature is $T = (3/2nk) \times \sum_{i=1}^2 \int d\mathbf{v}_1 (1/2) m_i (\mathbf{v}_1 - \mathbf{u})^2 f_i$, and the pressure is $P = P^{\text{HS}} + P^t$, where

$$P^{\text{HS}} = kT \left[n + \left(\frac{2\pi}{3} \right) \sum_{i,j=1}^2 \sigma_{ij}^3 y_{ij} n_i n_j \right], \quad (9)$$

and

$$P^t = \sum_{i,j=1}^2 a_{ij} n_i n_j. \quad (10)$$

$$a_{ij} = \frac{1}{2} \int_{\sigma}^{\infty} V_{ij}(\mathbf{r}) d\mathbf{r}. \quad (11)$$

The chemical potential is expressed as $\mu_i(T, \{n_j\}) = \mu_i^{\text{HS}} + \mu_i^t$, where

$$\mu_i^t = 2 \sum_{i,j=1}^2 a_{ij} n_j. \quad (12)$$

μ_i^{HS} is the chemical potential for component i in a binary mixture of hard spheres.⁴⁶

As mentioned, Eq. (6) can be solved on the basis of the method developed for hard-sphere mixtures presented in Ref. 21, with some appropriate changes. Hence, to follow the derivation given there, we will define some variables

$$K_i = 1 + (8\pi/5) \sum_{j=1}^2 \sigma_{ij}^3 y_{ij} n_j \mu_{ij} / m_{ij}, \quad (13)$$

$$K'_i = 1 + (8\pi/15) \sum_{j=1}^2 \sigma_{ij}^3 y_{ij} n_j \mu_{ij} / m_{ij}, \quad (14)$$

$$K''_i = 1 + P^{\text{HS}} / nkT + (4\pi/3) \sum_{j=1}^2 \sigma_{ij}^3 y_{ij} n_j \mu_{ij} / m_{ij}. \quad (15)$$

Now, Eq. (6) can be written in the following form:

$$\begin{aligned} & \sum_{j=1}^2 \sigma_{ij}^2 y_{ij} f_i^{(0)} \int d\mathbf{v}_2 f_j^{(0)} \int d\hat{\boldsymbol{\epsilon}} (\hat{\boldsymbol{\epsilon}} \cdot \mathbf{v}_{ji}) \Theta(\hat{\boldsymbol{\epsilon}} \cdot \mathbf{v}_{ji}) [\Phi_j(\mathbf{v}'_2) + \Phi_i(\mathbf{v}'_1) - \Phi_j(\mathbf{v}_2) - \Phi_i(\mathbf{v}_1)] \\ & = f_i^{(0)} \left[(\mathbf{v}_1 - \mathbf{u}) \cdot \left[K_i \left[\mathcal{C}_i^2 - \frac{5}{2} \right] \frac{\partial}{\partial \mathbf{r}} \ln T + \frac{n}{n_i} \mathbf{d}_i \right] + K'_i [2\mathcal{C}^{\circ} \mathcal{C}] \cdot \frac{\partial}{\partial \mathbf{r}} \mathbf{u} + \frac{2}{3} K''_i \left[\mathcal{C}_i^2 - \frac{3}{2} \right] \frac{\partial}{\partial \mathbf{r}} \cdot \mathbf{u} \right]. \end{aligned} \quad (16)$$

Equation (16) is the same as Eq. (25a) of Ref. 21. The only difference relies on the definition of \mathbf{d}_i , where the tail contribution is included. Hence, following the method of solution presented there,²¹ the independent mass flux in a binary system under the condition of no external forces, mechanical equilibrium and isothermal conditions can be obtained. This mass flux, relative to the local center of mass velocity, can be obtained by substituting the solution for the f_i to the first order in the gradients, into the expression

$$\mathbf{J}_i(r, t) = \int m_1 (\mathbf{v}_1 - \mathbf{u}) f_i d\mathbf{v}_1. \quad (17)$$

The most relevant steps of the derivation are presented in Appendix A. The final result is as follows:

$$\begin{aligned} \mathbf{J}_i^{(1)} = & -(\rho_i/2n^2) \sum_{j=1}^2 (1 - \delta_{jL}) \left[\sum_{k=1}^2 d_{i,0}^{(k)} \right. \\ & \left. \times (E_{kj} - (P_j/P_L) E_{kL}) \right] \frac{\partial}{\partial \mathbf{r}} n_j, \end{aligned} \quad (18)$$

where the $\mathbf{J}_i^{(1)}$ are the macroscopic mass fluxes to the first order in the gradients, relative to the local center of mass velocity, and

$$P_i = \sum_{j=1}^2 E_{ji},$$

and

$$E_{ij} = (n_i/k_B T) \left(\frac{\partial \mu_i}{\partial n_j} \right)_{T, n_{kj}}. \quad (19)$$

These functions defined in Ref. 21 should not be confused with the pressure.

Equation (18) has been written in such a way that all the gradients occurring in it are independent. The choice of component L , the dependent component, is arbitrary.⁴⁷ Although not explicitly indicated, the diffusion coefficients will depend on the choice of L . In the case of solutions, L is usually identified with the solvent.

The macroscopic isothermal-isobaric mass-diffusion coefficient for a binary system is defined by the relation

$$\mathbf{J}_i = - \sum_{j=1}^2 (1 - \delta_{jL}) D_{ij}^{\text{CM}} m_j \frac{\partial}{\partial \mathbf{r}} n_j. \quad (20)$$

In binary mixtures there is only one independent diffusion coefficient.¹ Equation (20) has been written in such a way that all the gradients occurring there are independent. Now, if Eqs. (18) and (20) are compared, one can obtain the expression for the MDC for the van der Waals binary mixture in the KVT I

$$D_{11}^{\text{CM}} = (\rho_1/2m_1 n^2) \sum_{j=1}^2 d_{1,0}^{(j)} [E_{j1} - (P_1/P_L) E_{jL}]. \quad (21)$$

Here the $d_{1,0}^{(k)}$ are the coefficients that appear in the Sonine polynomial expansion given by Eq. (A11). In order to obtain practical results, one restricts the number of Sonine polynomials in the expansion. We shall adopt here the convention usually called the N th Enskog approximation, i.e., only N Sonine polynomials are taken into account. For details see Appendix B. Equation (21) can be transformed straightforwardly into the expression given by Karkheck *et al.*⁴³ for the MDC. The dependence on the tail contribution in Eq. (21) comes through the chemical potential, Eqs. (12) and (19). The coefficients $d_{1,0}^{(j)}$ depend on the hard core part of the interaction only.

Although, our final formula is the same of that given by Karkheck *et al.*,⁴³ our procedure has an additional practical advantage. In our derivation, the explicit dependence of the tail contribution is handled in such a way that the structure of the equations given in Ref. 21 for the case of hard spheres is conserved. Thus the tail contribution is included into the chemical potential and the pressure. This makes easier the task of developing numerical solutions to calculate MDCs. In particular, comparisons between the KVT I and the RET are very simple, since we only need to turn off the tail contribution to recover the MDCs given in the RET.

Equation (21) can be used for calculating the MDC in binary mixtures, but if one is interested in comparisons with experimental MDCs of actual mixtures, some additional calculations are needed. From the experimental point of view, the natural MDCs are those given relative to the mean volume velocity. Therefore, a transformation is needed. The relationship between the MDC for a binary

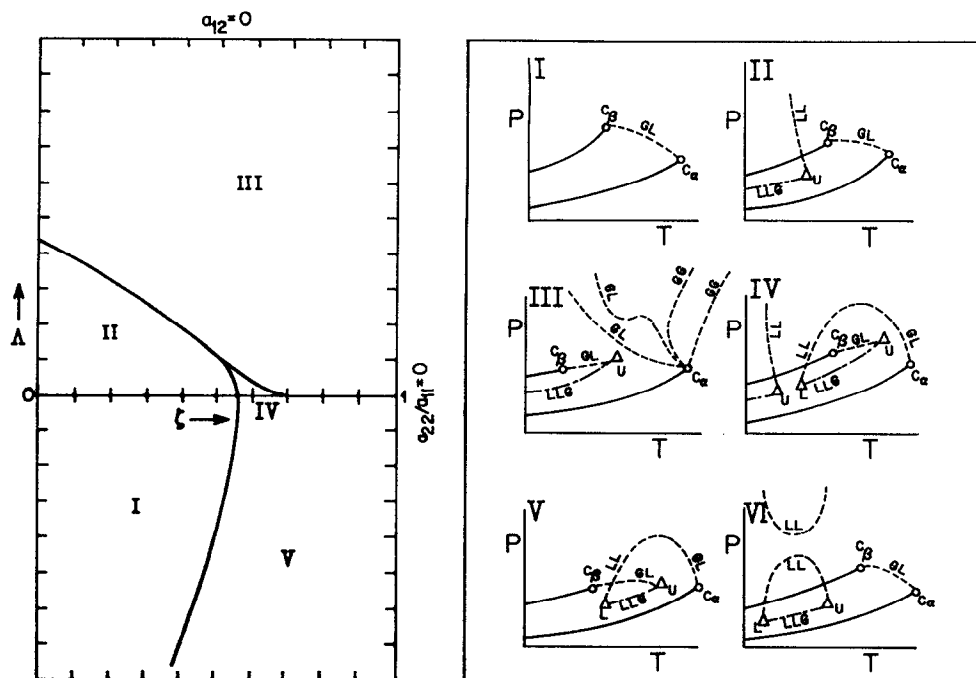


FIG. 1. Classification of Scott and van Konynenburg. (a) Values of Λ and ξ defining the main regions of similar phase diagram (modified from Ref. 33). The shield region is not shown. (b) Sketches of the pressure-temperature projections of the six possible types of fluid phase equilibria exhibited by binary mixtures [modified from K. E. Gubbins, K. S. Shing, and W. B. Street, *J. Phys. Chem.* **87**, 4573 (1983)]. The vapor-pressure curves of pure components are shown as solid curves. The gas-liquid-liquid three-phase lines are shown as dash-dot, and the gas-liquid and liquid-liquid critical lines are shown dashed. The U and L are the upper and lower critical end points, respectively.

mixture relative to the local center of mass velocity, D_{11}^{CM} , and to the mean volume velocity, D_{11}^V , is given by¹

$$D_{11}^V = (\rho v_2) D_{11}^{CM}, \quad (22)$$

where v_2 is the partial specific volume of component 2. For details see Appendix C.

III. FLUID PHASE EQUILIBRIA FROM THE VAN DER WAALS MODEL

Studies of fluid phase equilibria have shown that there are continuous transitions between phase diagrams that exhibit gas-liquid, liquid-liquid, and gas-gas phase separations. Critical lines are often observed to change continuously from one type of phase separation to another. When the lines representing a single degree of freedom (pure-component vapor pressure curves, three-phase lines, critical lines, etc.) are plotted on P - T diagrams, the resulting graphs fall naturally into several different categories, providing a convenient basis for classification of the fluid phase equilibria.

A very useful classification scheme has been devised some time ago by van Konynenburg and Scott,³³ who used the van der Waals equation of state in a systematic study of fluid phase equilibria. They characterized the mixtures by three dimensional parameters.

$$\xi = (b_{22} - b_{11}) / (b_{11} + b_{22}), \quad (23a)$$

$$\Lambda = \left(\frac{a_{22}}{b_{22}^2} - \frac{a_{11}}{b_{11}^2} \right) / \left(\frac{a_{11}}{b_{11}^2} + \frac{a_{22}}{b_{22}^2} \right), \quad (23b)$$

$$\Lambda = \left(\frac{a_{11}}{b_{11}^2} - \frac{2a_{12}}{b_{11}b_{22}} + \frac{a_{22}}{b_{22}^2} \right) / \left(\frac{a_{11}}{b_{11}^2} + \frac{a_{22}}{b_{22}^2} \right). \quad (23c)$$

For $\xi=0$, ζ is related to the difference in critical temperatures or pressures of the pure components, and Λ is related to the molar heat of mixing. The van der Waals constants a_m and b_m for the mixture depend upon mole fraction x_i as

$$a_m = \sum_{ij} x_i x_j a_{ij} \quad b_m = \sum_{ij} x_i x_j b_{ij}. \quad (24)$$

The constants a_{11} and a_{22} measure the attractive forces between pairs of molecules of the pure components 1 and 2, respectively, and a_{12} is the corresponding parameter for the interaction between molecules 1 and 2. The constants b_{11} , b_{22} , and b_{12} are the size parameters for the pure components and for mixed pairs, respectively. Here in agreement with the van Konynenburg and Scott convention,³³ we have used for the cross interaction

$$b_{12} = (b_{11} + b_{22}) / 2. \quad (25)$$

On the basis of selected parameters ξ and Λ , and of the P - T diagrams resulting from their calculations, van Konynenburg and Scott³³ grouped fluid phase equilibria diagrams into five types, see Fig. 1. As we can see in this figure, the diagrams were distinguished mainly by the configurations of the critical lines and the three-phase lines on P - T graphs. They recognized a sixth type of diagram that occurs in some aqueous systems, but it was not among those predicted by the van der Waals equation. In the di-

agrams of types I and II, the gas-liquid critical line is continuous between the critical points of the pure components, C_α and C_β . In the diagrams of type II, there is a liquid-liquid phase separation bounded by a three-phase region LLG and a liquid-liquid critical line LL; These two lines intersect at an upper critical end point. In the diagrams of type IV, the liquid-liquid-gas three-phase region is bounded above and below by critical end points. In the diagrams of type III, IV, and V, the gas-liquid critical line is divided into two or three branches. In the diagrams of type IV and V, the branch of the gas-liquid critical line originating in C_β terminates in an upper critical end point, while the branch originating in C_α rises to a maximum pressure and passes continuously into a liquid-liquid critical line, terminating in a lower critical end point. In the diagrams of type IV, there is a second liquid-liquid phase separation at lower temperatures, with a critical line ending in a second upper critical end point. Finally, in the diagrams of type III, the branch of the critical line originating in C_α rises to high pressures, sometimes passing through maximum and minimum pressures and/or a minimum in temperature.

The usefulness of the above described scheme lies in that it gives a qualitative description of the properties of the liquid mixtures, and very rarely yields non-physical results. Then, the fluid phase behavior that occurs in binary mixtures can be qualitatively discussed in terms of interaction parameters and changes of thermodynamic properties near the critical points. Therefore, a very natural extension of the work of van Konynenburg and Scott is to use this scheme to describe the behavior of diffusion coefficients of binary mixtures.⁴⁴

IV. MUTUAL DIFFUSION COEFFICIENTS FOR SYSTEMS OF TYPE I

The MDCs for several van der Waals liquid binary mixtures were calculated through Eqs. (21) and (22), in the third Sonine approximation. They were denoted by D_{11}^V . The parameters of the liquid mixtures were selected to fall into the diagrams of type I, of the van Konynenburg-Scott classification scheme. Here, we will present a numerical study to understand the influence of each parameter on the MDC. Moreover, several calculations for hard spheres are presented to clearly show the difference between the RET and the KVT I predictions.

There are several sets of parameters that can be used to define a binary mixture under study. We have used the following set: m_1 , m_2 , a_{22} , b_{22} , Λ , ξ , ζ , n , T , and X_2 . To make easier the interpretation of the results obtained in this numerical study, some of the mentioned parameters are fixed for most of the calculations. As a final goal, we shall use the procedure presented here to understand the behavior of the concentration dependence of the MDC for actual binary mixtures. Therefore, we selected the fixed parameters close to that of simple fluids, like liquid argon. These fixed parameters are $m_2 = 6.6335 \times 10^{-23}$ g, $a_{22} = 1.305$ L² at mol⁻², $b_{22} = 49.79 \times 10^{-3}$ L mol⁻¹, $T = 168$ K, $n = 2.03 \times 10^{22}$ L⁻¹. Changes in these parameters will be explicitly mentioned.

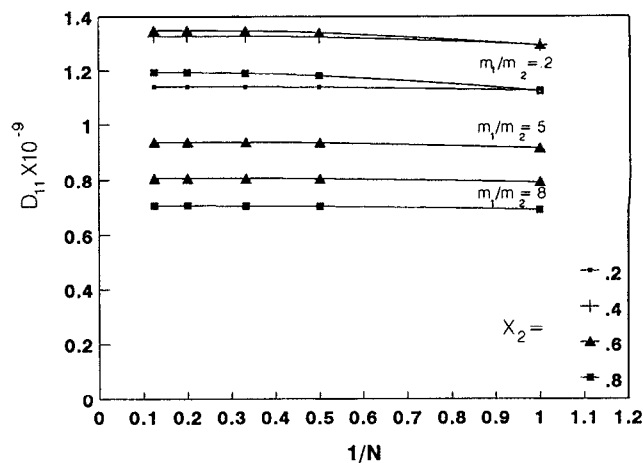


FIG. 2. The mutual diffusion coefficient as a function of the order N of the Enskog approximation for three values of the mass ratio m_1/m_2 , and four mole fractions ($\Lambda = -0.2$, $\xi = 0$, and $\zeta = 0$).

A first test of the theory was to show that the calculated coefficients, with respect to the mean volume velocity, have the property⁴⁷ that $D_{11}^V = D_{22}^V$. For this test, we calculated these diffusion coefficients along all the concentration range in the third Enskog approximation. The deviations between them never were greater than 0.01%.

Calculations with Eq. (21) are in the N th Enskog approximation, i.e., we are taking into account N Sonine polynomials in Eq. (A11). Hence, our second test was devoted to determine the most convenient Enskog approximation to be used in our calculations. Figure 2 shows the dependence of the MDC with the Enskog approximation for several mass ratios, and mole fractions ($\xi = 0$, $\zeta = 0$, $\Lambda = -0.2$). As we can see in Fig. 2, it is not necessary to calculate MDCs to an Enskog approximation greater than the third, since the error introduced is negligible. The calculations reported here will be in the third Enskog approximation.

Our next calculations were addressed to study the dependence of the MDC on the molecular mass. Here two hypothetical binary systems at several concentrations were studied (X_i denotes mole fraction of component i). The first one was made up of hard spheres, and the second one was made up of van der Waals molecules of type I ($\Lambda = -0.2$, $\xi = 0$, $\zeta = 0$). In both systems, the molecular volume was the same, as well as the temperature and the number density. Thus, the only difference between these two systems was the tail interaction. We studied these systems for three mass ratios, $m_1/m_2 = 0.25$, 1, and 4, but with a restriction: The total mass, $m_1 + m_2 = 6.6335 \times 10^{-23}$ g, should be a constant (in this case we changed the specified value for m_2 to fulfill the conditions required for this calculation). In Fig. 3, the calculations for the MDCs for both systems are presented, for each mass ratio. As we can see there, when the system is modeled as hard spheres the MDC is almost constant with respect to concentration changes. The total mass is the same for each case, whereas, there is an effect due to the asymmetry in the mass. The

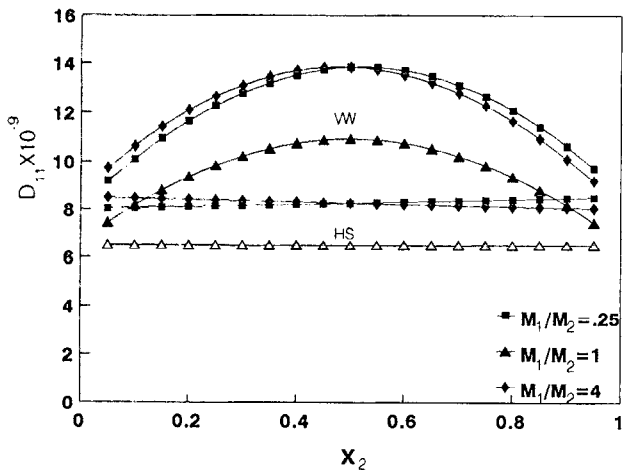


FIG. 3. The mutual diffusion coefficient as a function of the concentration (mole fraction) and the mass ratio m_1/m_2 . Here the total mass of the involved molecules is constant. The three upper lines are for van der Waals mixtures ($\Lambda = -0.2$, $\zeta = 0$, and $\xi = 0$), and the three lower lines correspond to hard-sphere mixtures.

more asymmetric the system, the higher the MDC. As far as we know, this effect has not been detected in the few simulation studies devoted to mutual diffusion in hard-sphere mixtures.^{23,24} The mass asymmetry behavior of the hard-sphere system is inherited by the van der Waals system. Here the MDC has a maximum at the middle of the concentration range due to the cross interaction. That will be discussed below. Figure 3 shows an additional test for our calculations, the curves corresponding for the ratios 0.25 and 4, are symmetric under a $m_1 \leftrightarrow m_2$ interchange.

Other interesting effects related to the mass are presented in Figs. 4 and 5. As above, we compared MDCs from a hard-sphere system and from a van der Waals system. The results for the hard-sphere system are presented in Fig. 4, and in Fig. 5 those for the van der Waals system. Now, we fixed the mass ratio ($m_1/m_2 = 0.8, 1$ and 1.25)

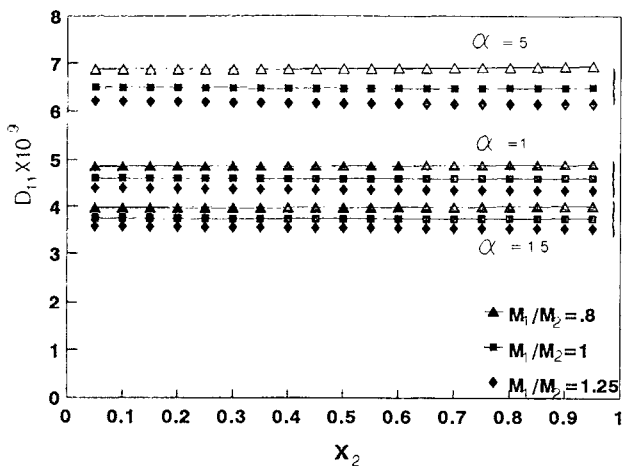


FIG. 4. The mutual diffusion coefficient for hard-sphere mixtures as a function of the concentration (mole fraction) and the mass ratio m_1/m_2 . Here the total mass of the involved molecules is not constant. $m = m_1 + m_2'$, with $m_2' = \alpha m_2$.

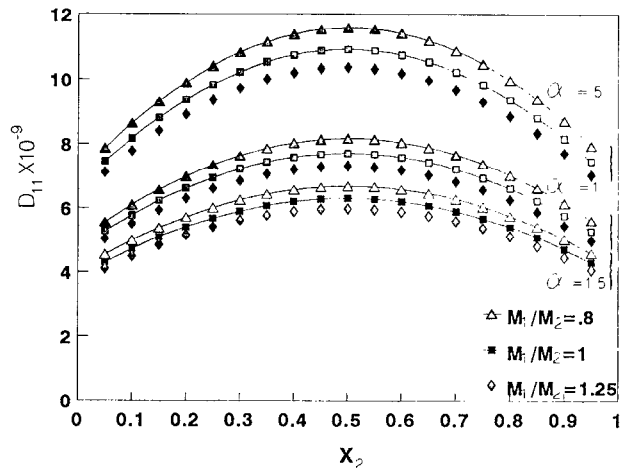


FIG. 5. The mutual diffusion coefficient for van der Waals mixtures ($\Lambda = -0.2$, $\zeta = 0$, and $\xi = 0$) as a function of the concentration (mole fraction) and the mass ratio m_1/m_2 . Here the total mass of the involved molecules is not constant. $m = m_1 + m_2'$, with $m_2' = \alpha m_2$.

and varied the total mass. The total mass was varied according to the formula $m = m_1 + m_2'$, with $m_2' = \alpha m_2$, where α can take the values 0.5, 1, and 1.5. In Fig. 4, as expected, the MDC goes down as the total mass of the molecules involved in the diffusion processes increases. This is particularly clear for the ratio $m_1/m_2 = 1$; here we have the same ratio, but the total mass is different ($m = m_2, 2m_2, 3m_2$). In the same way as before, when the tail interaction is included the same pattern of the hard-sphere case is obtained, but modified by the tail interaction. It is difficult to assure that this mass behavior of the MDC is the correct one. Computer simulations on hard-sphere mixtures do not help us to obtain a definite answer in this direction, since workers in this field have been interested in the diffusion of a single hard sphere in a hard-sphere fluid,^{48,49} or in other related topics.^{23,24} For other potential models, simulations have been performed for particles of equal mass.²⁹⁻³¹ For actual systems, there are specific studies to understand the effect of the molecular weight on the MDC.⁵⁰ Usually, they conclude that the diffusion coefficients decrease with the molecular weight. But in general, they include several effects at the same time, as volume effects and interaction effects. Hence, the actual aid of experimental data for understanding the role of the molecular mass is limited.

In Fig. 6, the effect of the cross interaction Λ on the MDC is presented for two mass ratios. Here the larger the cross interaction with respect to the interaction between like molecules (Λ is more negative), the larger the MDC. As mentioned in Sec. I, MDC measures the rate at which concentration fluctuations in the solution approach their equilibrium values. The decay of these fluctuations, to obtain the equalization of the concentration throughout the binary mixture, takes place by direct change of the composition of every small portion of the fluid. Thus the results presented in Fig. 6 are quite reasonable since Λ measures the preference of the molecules of the system to interact with unlike molecules, and to blend them. In Fig. 6, the

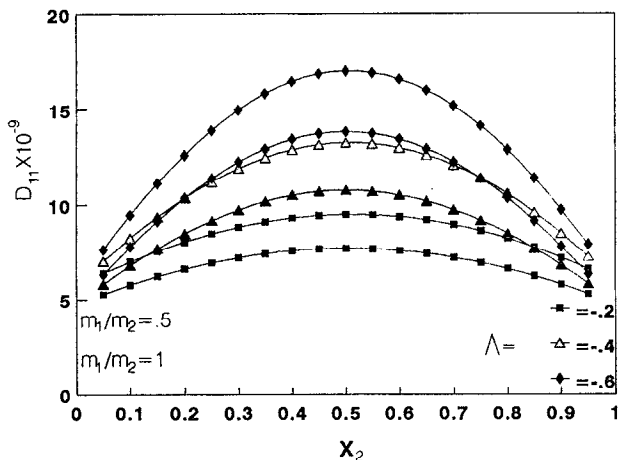


FIG. 6. The effect of the cross interaction on the mutual diffusion coefficient for the van der Waals mixture ($\xi=0$ and $\zeta=0$) for two mass ratios. The three upper lines are for $m_1/m_2=0.5$ and the three lower lines are for $m_1/m_2=1$.

$D_{11}-X_2$ curves have a maximum at $X_2=1/2$, because the mean interaction in the mixture has a maximum there, see Eq. (24) and (23c) for $\xi=0$. The described behavior can not be obtained with a hard-sphere system. Moreover, in Fig. 6 we can see how the total mass effect aids to increase the maximum of the $D_{11}-X_2$ curves. The MDC is larger for lighter particles.

The effect of changing the tail interactions between the particles of the fluid mixture can modify abruptly the $D_{11}-X_2$ diagrams. As an example, we present in Fig. 7 four different van der Waals binary mixtures corresponding to the diagrams of type I, where the value of a_{22} has been varied. The parameters defining these binary mixtures are $\Lambda=0$, $\xi=0$, $\zeta=0.3$, and $m_1/m_2=1$. Here it is very clear to see how the $D_{11}-X_2$ curves are modified as the value of the interaction parameter a_{22} is increased. Figure 7 suggests that, as a_{22} is increased, the system losses its capabil-

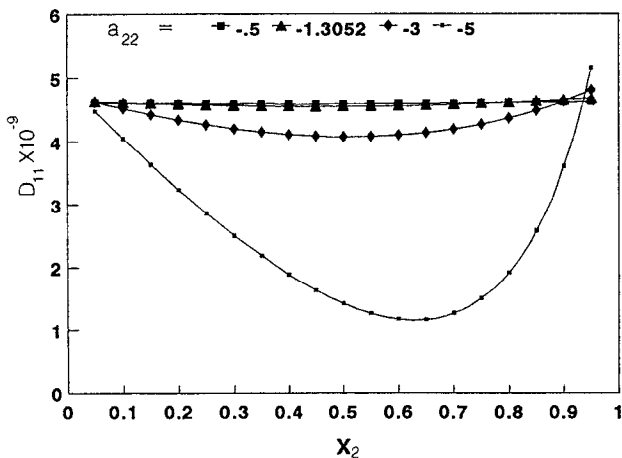


FIG. 7. The mutual diffusion coefficient for four van der Waals binary mixtures, where the value of a_{22} has been varied. The parameters defining the binary mixtures are $\Lambda=0$, $\xi=0$, $\zeta=0.3$, and $m_1/m_2=1$.

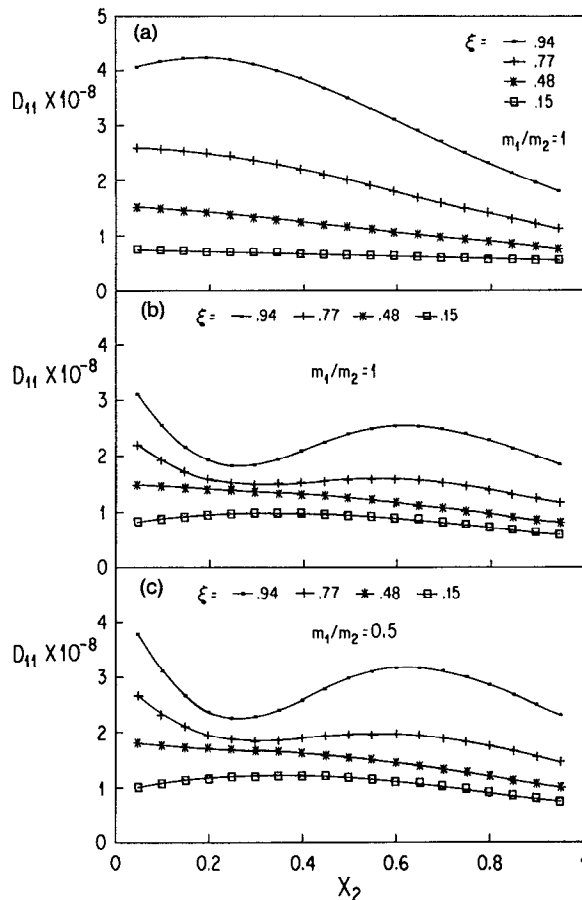


FIG. 8. The effect of the molecular volume on the mutual diffusion coefficient-concentration (mole fraction) curves. (a) Hard-sphere mixture. (b) van der Waals mixture with $m_1/m_2=1$ ($\Lambda=-0.2$ and $\zeta=0$). (c) van der Waals mixture with $m_1/m_2=0.5$ ($\Lambda=-0.2$ and $\zeta=0$).

ity to diffuse. Qualitatively our interpretation is as follows: For $\Lambda=0$, there is not enough cross interaction a_{12} . Thus, the mixture does not have a particular preference to mixing or demixing. However, as the interaction between molecules of compound 2 increases, the system response to the concentration fluctuations is to promote diffusion in the sense that the molecules of compound 2 can be, as far as possible, close together. Probably, this is the reason for which the minimum of the $D_{11}-X_2$ curves moves to the region rich in compound 2. After this minimum, the MDC grows with the mole fraction of compound 2 to facilitate the departure of molecules of species 1, during the concentration fluctuations, making possible to leave the system richer in compound 2.

The effect of the molecular volume can be obtained from Fig. 8. In Fig. 8(a), the MDCs for several binary hard-sphere systems as a function of the concentration are presented, for four values of $\xi=0.157, 0.489, 0.777$, and 0.947 . In all these cases the number density is constant. Here the MDC increases with the parameter ξ . This suggests that the diffusion process increases due to the motion of small molecules through the free space left by the larger molecules. At low ξ , we can see that the MDC decreases as the concentration of the larger component (2) goes to 1.

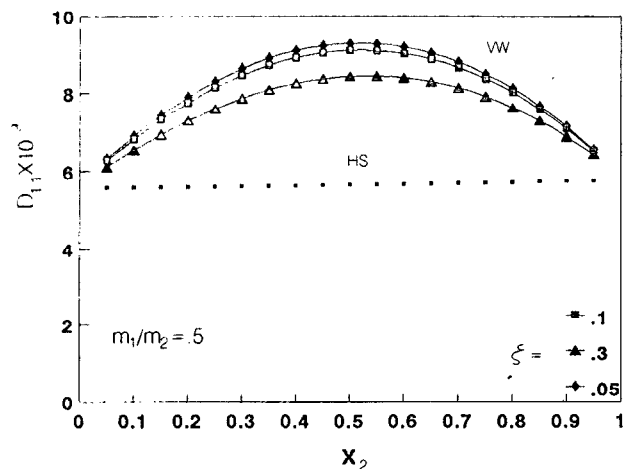


FIG. 9. The effect of the parameter ξ on the concentration dependence of the mutual diffusion coefficient using the KVT I (VW) and the RET (HS).

Since density is constant, the mixture has less molecules of component 1, thus the larger molecules have not enough room to diffuse. They block their motion themselves, like a cage effect. At greater values of ξ , Fig. 8(a) suggests that the diffusion of small molecules goes through the free space left by the larger molecules, and it can find a maximum at some specified concentration.

In Fig. 8(b), we have almost the same system as before in Fig. 8(a), i.e., have the same molecular volumes and ξ values, but now the molecules have tail interaction ($\Lambda = -0.2$, $\xi = 0$). Here as before the higher ξ , the higher MDC. This suggests that, diffusion through the holes left by the larger molecules is as important as in the hard-sphere system. Whereas, the situation in this case is more complicated, since we have two effects competing, the volume asymmetry and the cross interaction. At low ξ , the effect of the tail is dominant. But, at higher ξ both competing effects change completely the $D_{11}-X_2$ curve. It is quite suggestive in Fig. 8(b) that, the minimum in the curve corresponding to $\xi = 0.947$ occurs in the same region where the hard-sphere system has a maximum, due to the diffusion of the small molecules through the holes left by the larger molecules. When the attractive tails are turned on, the cross interaction between larger and smaller molecules must be more effective than at other concentration regions, probably due to the geometrical disposition of the hard cores. In this way the unexpected minimum of this curve can be explained. In Fig. 8(c) we present the same calculation as in Fig. 8(b), but for another mass ratio. The trend is similar although the MDCs are larger, since the total mass in this case is less than in the case shown in Fig. 8(b).

Figure 9 shows the dependence of the MDC on the parameter ξ for a van der Waals mixture of type I. Here it is clear that as the parameter ξ increases the MDC increases too, although, the effect of varying ξ is not very important. For comparison, we also present the same kind of calculations for a hard-sphere system obtained by turning off the attractive tails in the van der Waals mixture.

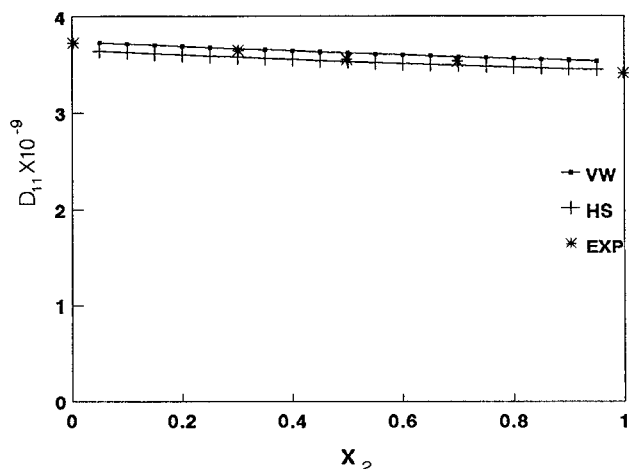


FIG. 10. Comparison between experimental mutual diffusion coefficients of hexane/heptane(2) (EXP) at 298.15 K, calculations using the van der Waals model (VW), and the hard-sphere theory (HS).

V. CALCULATIONS FOR ACTUAL MIXTURES

To evaluate the usefulness of our procedure in the case of actual binary mixtures, the MDCs of several mixtures were calculated. This test is possible only if experimental MDCs are provided for mixtures previously classified as belonging to the diagrams of type I in the van Konynenburg and Scott convention. Those selected were four:⁵¹ $\text{H}_2\text{O}/\text{D}_2\text{O}$,¹⁶ hexane/heptane,¹⁵ toluene/hexane,¹¹ and benzene/hexane.⁵² We performed calculations for those systems and the results are shown in Figs. 10–13 for several mole fractions. The interaction parameters used for these calculations are presented in Table I.

As expected, when predictions for actual fluids are performed, the most difficult problem is to obtain a reliable set of interaction parameters. Here an initial set of parameters was estimated as follows: each component was modeled as

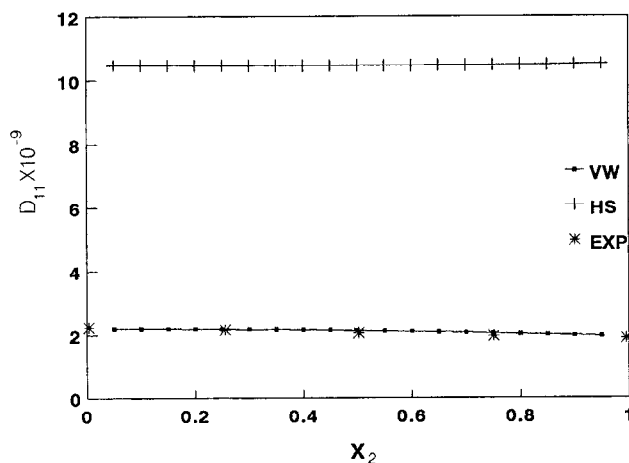


FIG. 11. Comparison between experimental mutual diffusion coefficients of $\text{H}_2\text{O}/\text{D}_2\text{O}(2)$ at 298.15 K (EXP), calculations using the van der Waals model (VW), and the hard-sphere theory (HS).

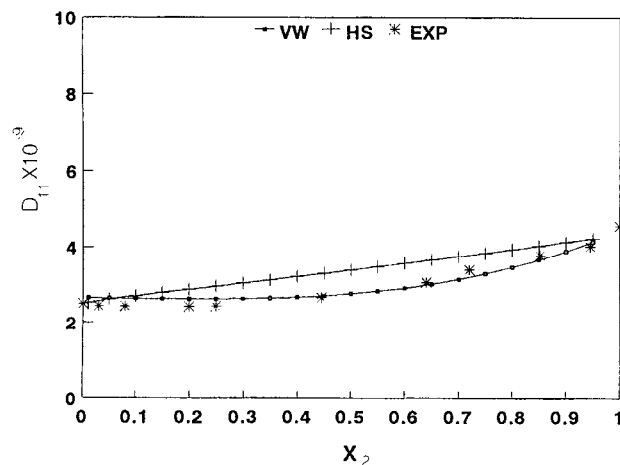


FIG. 12. Comparison between experimental mutual diffusion coefficients of toluene/hexane(2) at 298.15 K (EXP), calculations using the van der Waals model (VW), and the hard-sphere theory (HS).

a hard sphere of diameter σ (Lennard-Jones length parameter), plus an attractive Lennard-Jones tail. The a_{ii} 's and b_{ii} 's can be estimated through standard formulas.⁴⁶ The Lennard-Jones parameters, σ and ϵ , were obtained from Ref. 53. Since, our main interest was to understand how the different parameters affect to the $D_{11}-X_2$ curves, we were not interested in developing a procedure to obtain the best parameters that match the experimental data. Moreover, it is not known to what extent the correlated motion affect the MDC. Therefore, any intent of quantitative fitting can be misleading. Thus, the initial set of interacting parameters are modified for each mixture, in such a way that one can obtain the form of the experimental $D_{12}-X_2$ curves. In this way, we arrived to the final set of interacting parameters given in Table I. The cross interactions were selected in such a way that the binary mixtures ever fall into the region of the $\Lambda-\xi$ diagram corresponding to the

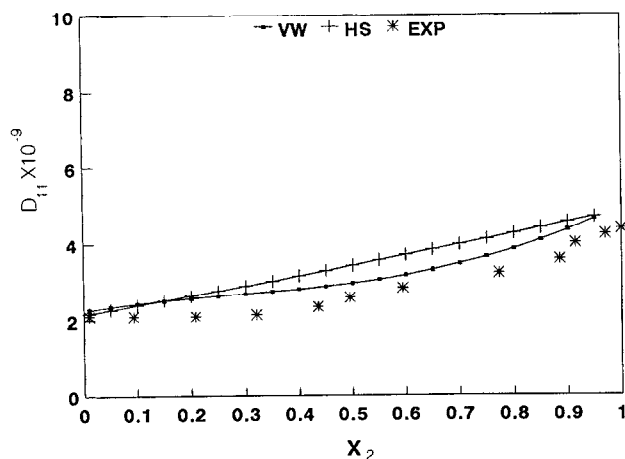


FIG. 13. Comparison between experimental mutual diffusion coefficients of benzene/hexane(2) at 293.15 K (EXP), calculations using the van der Waals model (VW) and the hard-sphere theory (HS).

TABLE I. Parameters for the actual mixtures.

	Hexane(1)/heptane(2)	H ₂ O(1)/D ₂ O(2)
a_{22}	30.0	4.05
b_{22}	319.0	26.23
Λ	-0.001	-0.001
ζ	0.0	0.0
ξ	0.1	0.004
	Benzene(1)/hexane(2)	Toluene(1)/hexane(2)
a_{22}	18.0	18.0
b_{22}	261.0	261.0
Λ	-0.001	-0.001
ζ	-0.53	-0.45
ξ	0.13	0.05

diagrams of type I (see Fig. 1). One important point to mention is that, the initial and the final sets of parameters are very close.

The different capability of the van der Waals model and of the hard-sphere model to predict the MDCs of actual mixtures can be compared. In the Figs. 10–13, calculations for the MDCs given in the RET were included, also in the third Enskog approximation. The hard-sphere diameters were exactly the same to those used for the van der Waals calculations, and Eq. (25) was used to define the volume cross interaction. The actual difference between the van der Waals and the RET calculations is the tail interaction.

Figures 10 and 11 present calculations for hexane/heptane and for of H₂O/D₂O, respectively. In both cases along all the concentration range. These examples suggest that the volume of the hard core interaction rules the behavior of the MDCs, since the cross interactions are almost zero. It is important to mention that our procedure predicts better the experimental data than the rough hard-sphere model.^{15,16}

Figure 12 presents calculations for toluene/hexane and Fig. 13 for benzene/hexane. In both cases along all the concentration range. We clearly see how the van der Waals model predicts qualitatively the same behavior as does the experimental data. For the case of toluene/hexane, the agreement with the experimental data is excellent. In general, the hard-sphere calculations cannot give the proper curvature shown by the experimental $D_{11}-X_2$ curves.

In summary, the results shown in this paper are encouraging. Here we have presented a model with attractive interaction where the MDC of binary liquid mixtures can be explicitly calculated. Moreover, within this model one is able to explain how the different parameters affect this coefficient. On the other hand, the procedure we have followed can be used to correlate experimental data of actual mixtures, and it requires very little input while still yielding reasonable qualitative good results. This procedure can be helpful to understand the MDC behavior of the remaining mixtures of the van Konynenburg Scott diagram. This study is underway and will be published shortly.

ACKNOWLEDGMENTS

We acknowledge partial support from DGAPAUNAM and CONACYT, Grants No. IN 102689 and 0114E, respectively. H.D. acknowledges DGAPA support for this work.

APPENDIX A: SOLUTION TO THE INTEGRAL EQUATIONS FOR Φ_i

Equations (16) are a set of two linear inhomogeneous integral equations for the Φ_i . These equations are soluble if the inhomogeneous part of the integral equations are orthogonal to the solutions of the homogeneous equations. However, the only solutions of the homogeneous equations are the conserved quantities in a binary collision. These conserved quantities are indeed orthogonal to the inhomogeneous part of Eqs. (16). Hence, one can find the solutions and they are fixed, apart from a linear combination of the solutions of the homogeneous equations. The solution of Eqs. (16) for the Φ_i can be made unique by using the following conditions:^{54,55}

$$\int f_i^{(0)} \Phi_i d\mathbf{v}_i = 0, \quad (\text{A1})$$

$$\sum_{i=1}^s \int f_i^{(0)} \Phi_i m_i \mathbf{v}_i d\mathbf{v}_i = 0, \quad (\text{A2})$$

$$\sum_{i=1}^s \int f_i^{(0)} \Phi_i m_i \mathbf{v}_i^2 d\mathbf{v}_i = 0. \quad (\text{A3})$$

Here, $\mathbf{V}_i = \mathbf{v}_i - \mathbf{u}$.

Equations (16) are linear in the gradients of the macroscopic quantities of different tensorial character, hence it is possible write the Φ_i as^{21,54,55}

$$\Phi_i = -\frac{1}{n} \left(\mathbf{A}_i \cdot \frac{\partial}{\partial \mathbf{r}} \ln T + \bar{\mathbf{B}}_i : \frac{\partial \mathbf{u}}{\partial \mathbf{r}} - H_i \frac{\partial}{\partial \mathbf{r}} \cdot \mathbf{u} + \sum_{k=1}^s \mathbf{D}_i^k \cdot \mathbf{d}_k \right). \quad (\text{A4})$$

Here we will restrict our derivation to obtain the MDC at constant temperature and pressure. This can be performed by substituting Eq. (A4) into $f_i = f_i^{(0)} [1 + \Phi_i]$, and the result must be substituted into the mass flux Eq. (17). Therefore, an expression for the mass flux in the first order of the gradients can be written in the form

$$\mathbf{J}_i^{(1)} = -\frac{m_i}{3n} \left[\sum_{j=1}^s \left(\int f_i^{(0)} \mathbf{D}_i^k \cdot \mathbf{V}_i d\mathbf{v}_i \right) \mathbf{d}_k \right]. \quad (\text{A5})$$

Now, the task is to calculate the integrals in the mass flux Eqs. (A5). If Eqs. (A4) are substituted into Eqs. (16), these integrals can be obtained through the following equations:⁵⁵

$$\begin{aligned} & \sum_{j=1}^2 \frac{\chi_{ij}}{n^2} \iint \sigma_{ij}^2 \Theta(\hat{\epsilon} \cdot \mathbf{v}_{ij}) (\hat{\epsilon} \cdot \mathbf{v}_{ij}) f_i^{(0)} f_j^{(0)} \\ & \times (\mathbf{D}_i^{k'} + \mathbf{D}_j^{k'} + \mathbf{D}_i^k + \mathbf{D}_j^k) d\hat{\epsilon} d\mathbf{v}_j = -\frac{f_i^{(0)}}{n_i} \left(\delta_{ik} - \frac{\rho_i}{\rho} \right) \mathbf{V}_i \\ & = \sum_{j=1}^s \frac{n_j}{n^2} I_{ij}(\mathbf{D}_i^k), \end{aligned} \quad (\text{A6})$$

where

$$\begin{aligned} I_{ij}(\mathbf{D}_i^k) &= \frac{\chi_{ij}}{n_i n_j} \iint \sigma_{ij}^2 \Theta(\hat{\epsilon} \cdot \mathbf{v}_{ij}) (\hat{\epsilon} \cdot \mathbf{v}_{ij}) f_i^{(0)} f_j^{(0)} \\ & \times (\mathbf{D}_i^{k'} + \mathbf{D}_j^{k'} + \mathbf{D}_i^k + \mathbf{D}_j^k) d\hat{\epsilon} d\mathbf{v}_j. \end{aligned} \quad (\text{A7})$$

An expression for Eqs. (A5) can be obtained, in terms of the bracket integrals,⁵⁵ if Eqs. (A7) are multiplied by a vector \mathbf{M} , then integrating over velocities and summing over i

$$\begin{aligned} & \int \sum_{i=1}^s \sum_{j=1}^s \frac{n_i n_j}{n^2} I_{ij}(\mathbf{D}_i^k) \mathbf{M}_i d\mathbf{v}_i \\ & = [\mathbf{D}_i^{(k)}, \mathbf{M}_i] = -\frac{1}{n_k} \int f_k^{(0)} \mathbf{M}_k \cdot \mathbf{V}_k d\mathbf{v}_k. \end{aligned} \quad (\text{A8})$$

Here the conditions to obtain a unique solution were used. In particular, for the case where $\mathbf{M}_i = \mathbf{D}_i^{(1)}$ the integrals given in Eq. (A8) are equal to those appearing in Eq. (A5). Thus, Eqs. (A5) can be written in the form

$$\mathbf{J}_i^{(1)} = -\frac{m_i}{3n} \left[\sum_{k=1}^s n_i [\mathbf{D}_i^{(k)}, \mathbf{D}_i^{(l)}] \mathbf{d}_k \right]. \quad (\text{A9})$$

An explicit expression for the bracket integrals can be obtained in terms of $\mathbf{D}_i^{(k)}(\mathbf{V}_i)$, if we take into account two facts. First, the integral operators of Eqs. (16) are isotropic in the velocity space, thus the \mathbf{D}_i^k are isotropic tensors in that space, i.e.,

$$\mathbf{D}_i^k(\mathbf{v}_i - \mathbf{u}) = D_i^k(|\mathbf{v}_i - \mathbf{u}|) (\mathbf{v}_i - \mathbf{u}). \quad (\text{A10})$$

Second, D_i^k can be expanded in terms of the Sonine polynomials in the following way:^{21,54,55}

$$D_i^{(k)}(\mathbf{V}_i) = \frac{m_i}{2kT} \sum_{r=0}^{\infty} d_{i,r}^{(k)} S_{3/2}^{(r)}(m_i V_i^2 / 2kT), \quad (\text{A11})$$

where $d_{i,r}^{(k)}$ are the Sonine coefficients, and $S_{3/2}^{(r)}$ are the Sonine polynomials.

To calculate the bracket integrals given in Eq. (A9), we need to substitute Eqs. (A10) and (A11) into Eq. (A8). Then, this result must be multiplied by $S_{3/2}^{(p)}$. A working expression can be found if the orthogonality properties of the Sonine polynomials are used, as well as conditions (A1)–(A3). (See Ref. 21 for details.) The bracket integrals for $\mathbf{D}_i^{(1)}$ can be written in terms of the Sonine coefficients in the form

$$[\mathbf{D}_i^{(k)}, \mathbf{D}_i^{(l)}] = -\frac{3}{2} d_{i,0}^{(k)}. \quad (\text{A12})$$

Equation (A9) can be written as

$$\mathbf{J}_i^{(1)} = \frac{\rho_i}{2n} \sum_{k=1}^2 d_{i,0}^{(k)} \mathbf{d}_k. \quad (\text{A13})$$

Finally, using the conditions

$$\sum_{i=1}^s \mathbf{d}_i = 0, \quad \mathbf{d}_i)_{T,P} = (n_i/n) \nabla \mu_i)_{T,P}, \quad (\text{A14})$$

and the Gibbs–Duhem equation, Eqs. (A13) can be handled in the form given in Eqs. (18).

APPENDIX B: EXPLICIT EXPRESSIONS FOR THE SONINE COEFFICIENTS

Substituting Eqs. (A12) and (A8) into Eq. (A7) enable us to obtain the Sonine coefficients given in Eq. (21). For details see Ref. 55. The equations obtained are

$$\sum_{j=1}^2 \sum_{q=0}^{N-1} \Lambda_{ij}^{pq} d_{j,q}^{(k)} = \frac{8}{25k} (\delta_{ik} - \rho_i/\rho) \delta_{p0}. \quad (\text{B1})$$

Here, the indexes are defined so that, $i=1, 2$, and $p=0, 1, 2, N-1$. N denotes the N th Enskog approximation. A expression for the Λ_{ij}^{pq} can be given as

$$[\]' = M_{nn'}^{(1)} = -\frac{\sigma_{ij}^{*2}}{2\pi} Q \sum_{p=0}^w \sum_{s=0}^{w-p} \sum_{m=0}^{w-p-s} \sum_{q=0}^1 \sum_{r=0}^{1-q} 4^p \frac{(r+s+p+q+1)!}{(p+q+1)!r!s!} \frac{\Gamma(n+n'-2s-2p-m-r-q+1/2)}{(n-m-s-p)!(n'-m-s-p)!(1-r-q)!m!} \times B_{pq}^{(1)} M_1^{(1+p-r-q)} M_2^{(n+n'+q-2m-2s-p)} (M_1 - M_2)^{(m+r+2s)}, \quad (\text{B5})$$

$$[\]'' = M_{nn'}^{(2)} = -\frac{\sigma_{ij}^{*2}}{2\pi} Q M_1^{(n'+1/2)} M_2^{(n+1/2)} \sum_{p=0}^w \sum_{q=0}^1 4^p \frac{\Gamma(n+n'-2p-q+1/2)}{(n-p)!(n'-p)!(1-q)!} B_{pq}^{(2)}, \quad (\text{B6})$$

with

$$B_{pq}^{(1)} = \frac{(2p+q+1)!}{2q!(2p+1)!} 2^{q-1} \frac{(p+q+1)!}{p!q!},$$

$$B_{pq}^{(2)} = \frac{(2p+q+1)!}{2q!(2p+1)!} \frac{1}{2} \delta_{p0} \delta_{q0},$$

$$Q = (2kT/M_{12})^{1/2}, \quad M_{12} = \frac{m_2 m_1}{m_1 + m_2}.$$

Here, $M_1 = [m_1/(m_1 + m_2)]$, $M_2 = [m_2/(m_1 + m_2)]$, and $w = \min(n, n')$.

$$\Lambda_{ij}^{pq} = \frac{8(m_i m_j)^{1/2}}{75k^2 T} \left\{ \delta_{ij} \sum_{l=1}^s \frac{n_l n_i}{n^2} [S_{3/2}^{(p)}(\mathcal{C}) \mathcal{C}^{1/2} \mathbf{v}, S_{3/2}^{(q)}(\mathcal{C}) \mathcal{C}^{1/2} \mathbf{v}]'_{il} + \frac{n_l n_j}{n^2} [S_{3/2}^{(p)}(\mathcal{C}) \mathcal{C}^{1/2} \mathbf{v}, S_{3/2}^{(q)}(\mathcal{C}) \mathcal{C}^{1/2} \mathbf{v}]''_{ij} \right\}, \quad (\text{B2})$$

where the bracket integrals []' and []'' are defined as follows:⁵⁴

$$[F, G]'_{ij} = \frac{1}{n_i n_j} \iiint f_i^{(0)} f_j^{(0)} G_i [F_i - F_i'] \theta(\mathbf{v}_{ij} \cdot \hat{\epsilon}) \times (\mathbf{v}_{ij} \cdot \hat{\epsilon}) \sigma_{ij}^{*2} d\hat{\epsilon} d\mathbf{v}_i d\mathbf{v}_j, \quad (\text{B3})$$

$$[F, G]''_{ij} = \frac{1}{n_i n_j} \iiint f_i^{(0)} f_j^{(0)} G_i [F_j - F_j'] \theta(\mathbf{v}_{ij} \cdot \hat{\epsilon}) \times (\mathbf{v}_{ij} \cdot \hat{\epsilon}) \sigma_{ij}^{*2} d\hat{\epsilon} d\mathbf{v}_i d\mathbf{v}_j. \quad (\text{B4})$$

here, $\sigma_{ij}^{*2} = \sigma_{ij}^2 \chi_{ij}$.

Equations (B1) are a set of linear equations. These can be solved in the N th Enskog approximation to find the Sonine coefficients $d_{i,0}^{(k)}$. Those coefficients can be obtained numerically solving the $N \times N$ determinant. The bracket integrals given in Eq. (B3) can be found through the transformation (B4).¹⁸ Under this transformation, the bracket integrals of Eqs. (B3) are identical to the bracket integrals of a dilute gas of hard spheres. Equation (B3) can be solved using the results of Ref. 56;

APPENDIX C: RELATIONS BETWEEN DIFFUSION COEFFICIENTS

Actual measurements of MDCs are usually performed with mass fluxes relative to the mean volume velocity. The MDC obtained from the kinetic equation, Sec. II Eq. (21), is given relative to the barycentric velocity. Hence, we must make a transformation between the fluxes to compare our calculations with experimental data. The transformation can be written in the form¹

$$\mathbf{J}^v = \rho v_2 \mathbf{J}^{cm},$$

where, v_2 is the partial specific volume, and ρ is the mass density. Here we follow the notation: v for quantities measured from the mean volume velocity, and cm from the barycentric velocity.

The partial specific volume is defined through¹

$$v_i = \left(\frac{\partial v}{\partial M_i} \right)_{T,P}, \quad (C1)$$

where M_i is the total mass of compound i . Then, Eq. (C1) can be handled in the form

$$v_i = \left(\frac{1}{m_i} \frac{\partial v}{\partial N_i} \right)_{T,P} = \left(\frac{1}{m_i} \frac{\partial \mu_i}{\partial P} \right)_{T,N_i}. \quad (C2)$$

Since $\mu_i = \mu_i(T, n_i)$, the derivative in Eqs. (C2) can be written the following form:

$$\frac{d\mu_i}{dP} = \frac{\partial \mu_i / \partial n_1 + \partial \mu_i / \partial n_2 (n_2/n_1)}{\partial P / \partial n_1 + \partial P / \partial n_2 (n_2/n_1)}, \quad i=1,2. \quad (C3)$$

$\partial \mu_i / \partial n_k$ and $\partial P / \partial n_k$ can be calculated from Eqs. (9) and (10), and (12) and from the hard-sphere expression of the chemical potential.⁴⁶

- ¹S. R. De Groot and P. Mazur, *Non-Equilibrium Thermodynamics* (Dover Publications, New York, 1944).
- ²H. J. V. Tyrrell and K. R. Harris, *Diffusion in Liquids* (Butterworths, London, 1984).
- ³L. S. Darken, *Trans. Am. Inst. Mining Met. Eng.* **175**, 184 (1949).
- ⁴G. S. Hartley and J. Crank, *Trans. Faraday Soc.* **45**, 801 (1949).
- ⁵P. A. Johnson and A. L. Babb, *Chem. Rev.* **56**, 387 (1956).
- ⁶P. C. Carman, *J. Phys. Chem.* **71**, 2565 (1967).
- ⁷S. J. Bertucci and W. H. Flygare, *J. Chem. Phys.* **63**, 1 (1975).
- ⁸K. J. Czorniak, H. Andersen, and R. Pecora, *Chem. Phys.* **11**, 451 (1975).
- ⁹H. L. Fiedman and R. Mills, *J. Solution Chem.* **10**, 395 (1981).
- ¹⁰W. Hess, G. Nagele, and A. Z. Akcasu, *J. Polym. Sci. B* **28**, 2233 (1990).
- ¹¹R. K. Ghai and F. A. L. Dullien, *J. Phys. Chem.* **78**, 2283 (1974).
- ¹²S. Chapman and T. G. Cowling, *The Mathematical Theory of Non-Uniform Gases* (Cambridge University, Cambridge, 1970).
- ¹³D. Chandler, *J. Chem. Phys.* **60**, 3500 (1974).
- ¹⁴S. F. Y. Li and L. S. Yue, *Int. J. Thermophys.* **11**, 537 (1990).
- ¹⁵C. M. Padrel de Oliveira, J. M. N. A. Fareira, and C. A. Nieto de Castro, *Int. J. Thermophys.* **10**, 973 (1989).
- ¹⁶M. L. S. Matos Lopes and C. A. Nieto de Castro, *Int. J. Thermophys.* **7**, 699 (1986).
- ¹⁷S. F. Y. Li and W. A. Wakeham, *Int. J. Thermophys.* **10**, 995 (1989).
- ¹⁸L. Barajas, L. S. Garcia-Colin, and E. Piña, *J. Stat. Phys.* **7**, 161 (1973).
- ¹⁹H. van Beijeren and M. H. Ernst, *Physica (Utrecht)* **68**, 437 (1973).
- ²⁰B. J. Alder, W. E. Alley, and J. H. Dymond, *J. Chem. Phys.* **61**, 1415 (1974).
- ²¹M. Lopez de Haro, E. G. D. Cohen, and J. M. Kincaid, *J. Chem. Phys.* **78**, 2746 (1983).

- ²²J. M. Kincaid, M. Lopez de Haro, and E. G. D. Cohen, *J. Chem. Phys.* **79**, 4509 (1983).
- ²³J. J. Erpenbeck, *Phys. Rev. A* **39**, 4718 (1989).
- ²⁴J. J. Erpenbeck, *Phys. Rev. A* **45**, 2298 (1992).
- ²⁵D. L. Jolly and R. J. Bearman, *Mol. Phys.* **41**, 137 (1980).
- ²⁶D. MacGowan and D. J. Evans, *Phys. Rev. A* **34**, 2133 (1986).
- ²⁷P. J. Gardner, D. M. Heyes, and S. R. Preston, *Mol. Phys.* **73**, 141 (1991).
- ²⁸S. Sarman and D. J. Evans, *Phys. Rev. A* **45**, 2370 (1992).
- ²⁹M. Schoen and C. Hoheisel, *Mol. Phys.* **52**, 33 (1984).
- ³⁰M. Schoen and C. Hoheisel, *Mol. Phys.* **52**, 1029 (1984).
- ³¹R. Vogelsang and C. Hoheisel, *Phys. Rev. A* **38**, 6296 (1988).
- ³²M. Kac, P. C. Hemmer, and G. E. Uhlenbeck, *J. Math. Phys.* **4**, 216 (1963).
- ³³P. H. van Konynenburg and R. L. Scott, *Philos. Trans. R. Soc. London*, **298**, 495 (1980); R. L. Scott and P. H. van Konynenburg, *Discuss. Faraday Soc.* **49**, 87 (1970).
- ³⁴D. Furman and R. B. Griffiths, *Phys. Rev. A* **17**, 1139 (1978).
- ³⁵J. W. Cahn and J. E. Hilliard, *J. Chem. Phys.* **28**, 258 (1958).
- ³⁶R. Evans, *Adv. Phys.* **28**, 143 (1979).
- ³⁷C. Varea, A. Valderrama, and A. Robledo, *J. Chem. Phys.* **73**, 6265 (1980).
- ³⁸C. Varea and A. Robledo, *J. Chem. Phys.* **75**, 5080 (1981).
- ³⁹K. Kawasaki, *Prog. Theor. Phys.* **41**, 1190 (1969).
- ⁴⁰B. Cichocki, *Physica* **75**, 157 (1974).
- ⁴¹J. Piasecki and P. Resibois, *J. Math. Phys.* **14**, 1984 (1973).
- ⁴²P. Resibois, Y. Pomeau, and J. Piasecki, *J. Math. Phys.* **15**, 1238 (1974).
- ⁴³J. Karkheck, E. Martina, and G. Stell, *Phys. Rev. A* **25**, 3328 (1982).
- ⁴⁴R. Castillo, M. E. Costas, and A. Robledo, *Int. J. Thermophys.* **10**, 427 (1989).
- ⁴⁵G. Stell, J. Karkheck, and H. van Beijeren, *J. Chem. Phys.* **79**, 3166 (1983).
- ⁴⁶T. M. Reed and K. E. Gubbins, *Applied Statistical Mechanics* (McGraw-Hill, New York, 1973).
- ⁴⁷D. D. Fitts, *Nonequilibrium Thermodynamics* (McGraw-Hill, New York, 1962).
- ⁴⁸P. T. Herman and B. J. Alder, *J. Chem. Phys.* **56**, 987 (1972).
- ⁴⁹G. Subramanian, D. Levitt, and H. Davis, *J. Chem. Phys.* **60**, 591 (1974).
- ⁵⁰E. Grushka and E. J. Kikta, *J. Am. Chem. Soc.* **98**, 643 (1976).
- ⁵¹J. S. Rowlinson, and F. L. Swinton, *Liquids and Liquids Mixtures* (Butterworths Scientific, London, 1982).
- ⁵²W. Kranh, G. Schwegler, and K. Lucas, *J. Phys. Chem.* **87**, 4515 (1983).
- ⁵³R. C. Reid, J. M. Prausnitz, and T. K. Sherwood, *The Properties of Gases and Liquids*, 3rd ed. (McGraw-Hill, New York, 1979).
- ⁵⁴C. Cercignani, *The Boltzmann Equation and its Applications* (Springer, New York, 1988).
- ⁵⁵J. H. Ferziger and G. H. Kaper, *Mathematical Theory Of Transport Process in Gases* (North Holland, Amsterdam, 1972).
- ⁵⁶M. J. Lindenfeld and B. Shizgal, *Chem. Phys.* **41**, 81 (1979).